Author/s:
Devnani, B;Ong, L;Kentish, S;Gras, SL

Title:
Structure and functionality of almond proteins as a function of pH

Date:
2021-10-01

Citation:
Devnani, B., Ong, L., Kentish, S. & Gras, S. L. (2021). Structure and functionality of almond proteins as a function of pH. Food Structure, 30, https://doi.org/10.1016/j.foostr.2021.100229.

Persistent Link:
https://hdl.handle.net/11343/336907

Structure and functionality of almond proteins as a function of pH

Bhanu Devnani[a.b], Lydia Ong[a,b], Sandra Kentish[a] , Sally Gras[a,b]

[a]*Department of Chemical Engineering, The University of Melbourne, Parkville, Victoria 3010, Australia*

[b]*The Bio21 Molecular Science and Biotechnology Institute, The University of Melbourne, Parkville, Victoria 3010, Australia*

*Corresponding author: Email- sgras@unimelb.edu.au, Ph- +613 8344 2259

Abstract

Almond proteins have potential utility in a range of food and beverages but it is not clear how pH affects protein structure and function. The behaviour of almond protein isolate was examined under conditions of neutral and acidic pH (pH 7 and 4). The isolate was highly soluble (70-80 %) at either pH. An increase in acidity lead to protein unfolding, an increase in random coil structure and the appearance of lower molecular weight proteins due to acidic hydrolysis. These structural changes at pH 4 increased the capacity for foam formation and foam stability, increased viscosity and led to concentration and age dependent thickening. Gels, similar in strength but with distinct microstructures and properties were obtained following heating. At pH 7, a particulate type gel with an interconnected protein network was formed, while the gel at pH 4 had a dense continuous protein matrix. The gels differed in their susceptibility to chemical disruption, suggesting different underlying molecular interactions. The ability to alter protein structure and properties as a function of pH and heating could be used to broaden the application of almond proteins and develop a variety of food products, such as protein supplements and vegan alternatives to traditional products.

Keywords: Almond proteins, pH, acid hydrolysis, age-thickening, gelation

1. Introduction

Almonds are highly versatile, nutrient-dense nuts that offer a large proportion of heart healthy fats (25-66 %), good quality proteins (14-26 %) and few carbohydrates (2-8 %) (Summo, et al., 2018; Yada, Lapsley, & Huang, 2011). They have high economic value but also a known environmental impact and high water footprint (~12 litres/almond) (Fulton, Norton, & Shilling, 2019; Kendall, Marvinney, Brodt, & Zhu, 2015). Almonds have traditionally been used in the food industry within confectionary, snack, bakery, bar and cereal products. Due to increasing consumer interest in plant-based diets, new product areas have come into focus in the past few years, including almond-based dairy alternatives, spreads and protein powders. Almond protein quality (44.3–47.8), as assessed by the protein digestibility amino acid score (PDCAAS), is similar to that of other plant-based nut, cereal and seed proteins, such as walnuts (51), wheat (40) and hemp seeds (46-51), with lysine being the limiting amino acid in all these products (House, Hill, Neufeld, Franczyk, & Nosworthy, 2019). The combination of lysine deficient proteins with legume proteins offers a complementary amino acid profile and can be used to enhance the overall PDCAAS score (Boye, Wijesinha-Bettoni, & Burlingame, 2012; House, et al., 2019).

Although some literature suggests that the majority (80-95 %) of almond proteins are water soluble, this figure could be as low as ~50 % of the total proteins present and depends on the method used for analysis (Calixto, Canellas, & de Toda, 1982; Sathe, 1992; Sharma, Su, Joshi, Roux, & Sathe, 2010). The protein extract isolated with water is least soluble between pH 3-5 and is dominated by the major almond storage protein, known as amandin, which constitutes 65-70 % of the total soluble protein (Wolf & Sathe, 1998). Amandin is a classical globulin characterised by a sedimentation coefficient of 14S, molecular weight of 360 kDa with a hexameric structure composed of 6 prunin sub-units, each having a molecular weight of ~60-66 kDa (Albillos, et al., 2008; Sathe, 1992; Wolf, et al., 1998). In the presence of a reducing agent, each prunin subunit dissociates into its acidic and basic polypeptides, with molecular masses of ~42 kDa and ~20 kDa (Wolf, et al., 1998). The majority of almond proteins, including amandin, are known to have allergenic potential (Costa, Mafra, Carrapatoso, & Oliveira, 2012) and are highly stable towards common processing treatments, such as blanching and dry roasting (Su, Liu, Roux, Gradziel, & Sathe, 2017). A recent study demonstrated, however, that autoclaving could successfully reduce the immunoreactivity of

almond proteins, potentially by inducing structural changes that reduced the availability of antigen binding epitopes (De Angelis, Bavaro, Forte, Pilolli, & Monaci, 2018).

To date, only a few studies have evaluated the functional properties of almond proteins. In the pH range of 5 to 6.46, almond protein isolate (API) exhibits either comparable or better foaming and emulsification properties than soy protein isolate on a weight for weight basis (Sze-Tao & Sathe, 2000). Recent studies have reported the emulsification and foaming properties of different almond extracts over a broad range of pH (2-10), with these properties varying across studies, perhaps due to different almond varieties and methods of protein extraction (Amirshaghaghi, Rezaei, & Rezaei, 2017; de Souza, Dias, Koblitz, & de Moura Bell, 2020).

Limited information is available on the viscosity of API and the properties of gels formed from these proteins. At near neutral pH (6.46), API has a low viscosity and behaves as a non-Newtonian shear thinning fluid (Sze-Tao & Sathe, 2000; Zhang, Zhang, Feng, & Shi, 2017). Protein denaturation and gelation has been observed when almond proteins in the pH range 6.2-8.2 are subjected to heat treatment, with the concentration for minimum gelation depending on the system examined (3.6 % for almond milk (Devnani, Ong, Kentish, & Gras, 2020), 4 % for API (Sathe & Sze, 1997) and 8 % for defatted almond flour (Joshi, Liu, & Sathe, 2015)). The properties of almond proteins, including structural stability and viscosity, under acidic conditions are not known. The effect of combining acidic conditions and heat treatment on the properties and gelation of almond proteins is also not understood. Yet, such information is important if almond proteins are to be more broadly applied in newly emerging areas such as protein supplements, ready to drink beverages, which may be protein fortified and acidic with a pH ranging from 2.5-4.5 or near neutral pH, as well as plant-based milk alternatives and drinkable yoghurts. The demand for high protein vegan gelled products, including yoghurt and cheese alternatives, has also fuelled the need to explore and characterise the gels formed by almond proteins under acidic and near neutral conditions.

This study aimed to explore the fundamental and functional properties of almond proteins at acidic conditions and compare these properties to those found at neutral pH and to better understand the properties of gels formed by almond proteins. The functional properties studied included thermal stability, foaming, viscosity and heat-induced gelation, which are important for beverage and food applications and may have broader applicability in personal care or nutraceutical products. Non-pareil almonds, the most dominant almond variety grown world-

wide (Almond Board of California, 2020), were utilised for this study, as the functional properties of almond proteins are known to vary as a result of variety.

2. Materials and Methods

2.1 Materials and reagents

Raw whole Australian Nonpareil almonds were bought from Woolworths Supermarket, Melbourne, Victoria. Purified water (Millipore Type 3, resistance >18.2 MΩ.cm at 25 °C, Merck Millipore Corporation, Bedford, MA), was used for all experiments. All chemicals (analytical grade) were purchased from Chem Supply (Gillman, SA, Australia) unless otherwise stated.

2.2 Preparation and compositional analysis of almond protein isolate

Almond protein isolate (API) was produced using a two-step process. In the first step, raw almonds were ground and defatted to obtain defatted almond flour, which was then solubilised in borate saline buffer to extract almond proteins.

Defatted almond flour was obtained following the process of Albillos, Menhart, and Fu (2009), with minor modifications. Briefly, raw almonds were ground in a MultiGrinder (Sunbeam Corporation, NSW, Australia) to obtain almond flour, which was defatted with hexane at room temperature with a flour to solvent ratio of 1:10 (w/v) through continuous shaking at 250 rpm for 3 hours. This slurry was then vacuum filtered through Whatman filter paper number 4 and the residue obtained was defatted again under similar conditions. After the completion of the two-stage defatting process, the almond flour-hexane slurry was left in the fume hood overnight to remove the residual hexane. The defatted almond flour was homogenized in a MultiGrinder, passed through a 40-mesh sieve and stored at room temperature (25 ºC).

The method of Sharma, et al. (2010) was used for the preparation of API due to its potential to achieve a higher protein yield compared to conventional alkaline extraction (Sathe, et al., 2009). Almond proteins were extracted from the defatted almond flour using saline borate buffer (0.1 M H_3BO_3, 0.025 M $Na_2B_4O_7$, 0.075 M NaCl, pH 8.45) with a flour to solvent ratio of 1:10 (w/v) with constant magnetic stirring for 2 hours. The slurry was centrifuged at 15000 g for 30 minutes and the supernatant filtered through Whatman filter paper number 4. The filtrate was then concentrated using 3 kDa centrifugal filters and the concentrate was dialysed against distilled water for 48 hours at 4 ºC. After dialysis was complete, the protein solution was freeze-dried and stored in airtight bottles at -20 ºC until further use.

The chemical composition of raw almond flour and almond protein isolate was analysed. To measure the moisture content, samples were placed in an oven at ~105 °C until a constant weight was achieved (Method 1990.20, (AOAC, 2016)). The fat content was determined using a Soxhlet apparatus with hexane as a solvent (Method 948.22, (AOAC, 2016)).The protein was quantified by nitrogen analysis through the Dumas combustion method (AOAC 968.06, (AOAC, 2016)) using a Leco TruMac CNS Macro Analyser (LECO Corporation, Michigan, USA). A nitrogen to protein conversion factor of 5.18 was used. Protein yield was calculated using the following equation:

$$\text{Protein yield} = \frac{\text{Total weight of protein isolate}}{\text{Total weight of defatted almond flour}} * 100 \quad (1)$$

2.3 Preparation of protein solutions

Protein solutions were prepared at room temperature by dispersing almond protein isolate in purified water, 0.01 M acetate buffer (pH 3-5), 0.01 M phosphate buffer (pH 6-8) or 0.01 M borate buffer (pH 9) at the concentration required for analyses, allowing ~30 minutes for dissolution of the protein. After the dissolution was complete, some solutions prepared in purified water were then pH adjusted to 4 and/or 7 using 1 M HCl or 1 M NaOH. All the measurements were performed after solutions were equilibrated for 24 hours at room temperature, unless otherwise specified. Sodium azide (0.02 %) was added to all solutions to prevent microbial growth.

2.4 Fundamental properties

2.4.1 Solubility

For solubility measurements, water-based protein solutions (9 % w/w protein) with pH values ranging from pH 3 to pH 9 were prepared. After ~ 30 minutes, the solutions were centrifuged at 16000 g for 10 minutes. The supernatants obtained were then completely dried in Nickel liners at 105 °C and the soluble protein was quantified using the Dumas combustion method, as described in Section 2.2. Protein solubility is reported as the percentage soluble protein present in the supernatant after centrifugation with reference to the total protein present in the dry powder.

2.4.2 Zeta potential

The Zeta potential of the protein suspended in buffer (1 mg/mL) at each pH following centrifugation at 16000 g for 10 minutes, was determined with a Zetasizer Nano ZS (Malvern Panalytical Ltd, Malvern, UK), based on the principle of laser Doppler micro-electrophoresis, using a DTS 1070 cuvette. All measurements were conducted in triplicate and the results are expressed as average values obtained from three independent measurements (n=3 ± the standard deviation).

2.4.3 Circular dichroism spectroscopy

The circular dichroism (CD) spectra of protein solutions (0.2 mg/mL) prepared in pH 4 and pH 7 buffer were obtained at room temperature with an AVIV CD-spectrometer (Biomedical Inc., New Jersey, USA) using a cuvette with a path length of 1 mm. The spectral resolution and bandwidth were set at 1 nm and data collection interval was 1 s. Spectra were collected three times for each protein sample on two different occasions (n=2 ± the standard deviation).

The approximate composition of secondary structure i.e. α-helix, β-sheet and unordered structure in the unheated protein solutions was estimated by deconvoluting the spectral data using CONTIN-LL, SELCON 3 and CDSSTR algorithms available through Dichroweb (Whitmore & Wallace, 2004) and the data expressed as a percentage. The largest reference set (Set 7) with 48 different proteins was chosen for this analysis (Sreerama & Woody, 2000). As suggested by Sreerama, et al. (2000), results obtained from different algorithms were averaged and compared for better reliability.

2.4.4 SDS-PAGE Electrophoresis

The molecular weight distribution of the proteins present in the supernatants after centrifugation (as prepared in Section 2.4.2) was analysed by electrophoresis using the method of Laemmli (1970), under both non-reducing and reducing conditions, within ~2 hours of preparation of the protein solution. A pre-cast 4-12 % gradient Tris Glycine gel was used with the apparatus from Bio-Rad laboratories (Bio-Rad, Richmond, CA, USA). Samples without reducing agent were produced by adding 5 µL of 4X Bolt LDS sample buffer (Thermo Fisher Scientific) to 15 µL of each supernatant. To produce reduced samples, a 2 µL aliquot of 10X Bolt reducing agent (Thermo Fisher Scientific) was also added to 13 µL of each supernatant, in addition to 5 µL of 4X Bolt LDS sample buffer. Each sample (12 µL) was loaded and the gels run using a Tris glycine/SDS running buffer, with a voltage of 125 V, until the tracking dye reached the bottom of the gel. A solution of 2.5 g/L Coomassie brilliant blue (R-250) in 7.5 % (v/v) acetic acid and 40 % (v/v) methanol solution was used for staining the gel and a

solution of 7.5 % (v/v) acetic acid used for de-staining the gel. Bio Rad markers were run in parallel with the samples (Precision Plus pre-stained dual colour protein standards, Bio-Rad). SDS-PAGE analysis was performed three times (n=3) and one representative gel is presented.

2.5 Functional properties

2.5.1 Thermal denaturation

Differential scanning calorimetry was used to study temperature induced unfolding of almond proteins, as this technique can provide detailed information about the temperature of denaturation for protein mixtures (Gill, Moghadam, & Ranjbar, 2010). A Nano DSC differential scanning calorimeter (TA Instruments, New Castle, USA), fitted with capillary cells, was used to detect the thermal transition of proteins in solution at pH 4 and pH 7. Approximately, 600 μL of water or 1% (w/v) pH adjusted water-based protein solution was loaded in the reference and the sample capillary cell respectively. The system was then pressurized to 3 atm and solutions heated from 25 ºC to 120 ºC at a rate of 2 ºC/minute. Measurements were performed on three independently produced protein solutions and the results averaged for each pH (n=3 ± the standard deviation).

2.5.2 Foaming properties

Differences in foaming capacity and foam stability at pH 4 and pH 7 were tested following the method of Aluko and colleagues (Aluko, Mofolasayo, & Watts, 2009) using 1% (w/v) protein solutions in pH adjusted water. In a 25 mL measuring cylinder, 10 mL of protein solution at each pH was homogenized at 19,400 g for 30 seconds at room temperature using a Polytron PT-K homogeniser (Kinematica AG, Luzern, Switzerland) fitted with a 10-mm probe. The percentage volume increase after homogenisation was taken as the foaming capacity.

Foam stability was reported as the percentage decrease in foam height with time. Foam height was noted at time intervals of 15 minutes up to 1.5 hours. Three replicates were prepared, and the data reported are the average each pH (n=3 ± the standard deviation).

2.5.3 Viscosity

Solutions with 3 %, 6 % or 9 % protein (3.16 %, 6.32 % and 9.48 % Total Solids), 10 mL in volume, were prepared in 15 mL centrifuge tubes with purified water and the pH adjusted to 4 or 7. Immediately after pH adjustment, the solutions were vortexed for one minute. To minimise the extent of foam formation and its subsequent effect on rheological measurements, the samples were vortexed at the lowest speed of ~200 rpm provided by the Corning LSE

Vortex mixer 6776 (Corning Inc, New York, USA). Samples were withdrawn from the lower section of the tube avoiding any foam. The samples were then placed on a Discovery HR-2 Hybrid rheometer (TA Instruments, New Castle, USA). Flow curves were obtained using a cone and plate test geometry (40 mm diameter, 2º angle) with a geometry gap of 58 µm. The temperature was maintained at 25 ºC by a Peltier temperature control unit and a water thermo-circulator. The samples were equilibrated to 25 ºC within 60 s and sheared between $0.01 s^{-1}$ to $100\ s^{-1}$ for 5 minutes.

Changes in apparent viscosity were measured at room temperature (~25 ºC) for a period of 72 hours for solutions having protein concentrations of 3 % or 6 % (w/v); and 24 hours for solutions having protein concentration of 9 % (w/v), with added Na azide (0.02%) to prevent microbial growth. The flow curves obtained for each protein concentration at each time point were fitted to a power law; $\eta = k\dot{\gamma}^{n-1}$, where η, k, $\dot{\gamma}$ and n represent viscosity (Pa.s), consistency coefficient ($Pa.s^n$), shear rate (s^{-1}) and flow behaviour index (dimensionless). Apparent viscosity values at a shear rate of $1\ s^{-1}$ (or the consistency index K) were plotted against time. All measurements were conducted in duplicate and results are expressed as the average obtained from solutions made on three different occasions (n=3 ± the standard deviation).

2.5.4 Gelation and gel microstructure

Temperature sweep tests were conducted using 9% (w/v) protein solutions that had been pH adjusted using a Discovery HR-2 Hybrid rheometer (TA Instruments). A cone and plate test geometry (40 mm diameter) with a geometry gap of 1000 µm was used for this purpose. The samples were heated from 25 ºC to 90 ºC at a rate of 3 ºC/minute at a constant frequency (1 Hz) and strain (1%; within the linear viscoelastic region) and then cooled to 25 ºC, where the temperature was again controlled with a water thermo-circulator and a Peltier temperature control unit. To prevent water evaporation, a two-piece solvent trap cover was used. The gelation temperature for liquid protein solutions at pH 7, was defined as the temperature where the storage modulus G' became greater than the loss modulus G". Temperature sweeps were carried out on three independently made protein solutions and the data averaged (n=3 ± the standard deviation).

The microstructure of almond protein solutions/ gels formed before and after the temperature sweeps at both pH 4 and pH 7 was studied at room temperature using an inverted confocal laser scanning microscope (CLSM, Leica SP8, Leica Microsystems, Heidelberg, Germany) following the protocol developed by Ong, Dagastine, Kentish, and Gras (2011). Fast green FCF

(0.1 %) and Nile red (0.1 %) solutions were used to stain protein and fat respectively. Briefly, for liquid samples, 10 µL of each staining solution was added to 480 µL of protein solution and the mixture vortexed. This stained protein solution (50 µL) was then mixed with 200 µL of lukewarm (~40 ºC) agarose solution (0.5%). A 5 µL aliquot of this mixture was then transferred to a cavity slide (ProSciTech, Thuringowa, Queensland, Australia) which was covered with a 0.17 mm thick glass coverslip (ProSciTech) fixed with nail polish. The agarose solution forms a gel at room temperature, preventing Brownian motion in liquid samples during imaging. For gel samples, a thin section of the gel was cut and placed on a slide. The gels were then stained with staining solutions mentioned above but diluted 5 times.

Single optical sections (1024×1024 pixels) were acquired for each sample using a ×63 magnification objective. Dual-channel images were obtained using excitation at 488 nm and 633 nm to visualise the protein and fat, respectively.

2.5.5 Molecular interactions in gel formation

The molecular interactions involved in gel formation were evaluated using the method of Yang, Wang, Vasanthan, and Chen (2014) with some modifications. Almond protein gels, 3 mm in thickness, were prepared by heating 5 mL of 9 % (w/v) protein solutions in tightly capped tubes (3 cm in diameter) in a water bath for a total duration of 30 minutes. A Center 309 Data Logger thermometer (CENTER Technology Corp., New Taipei City, Taiwan) was used to record the change of temperature with time. The temperature achieved in the samples after 7 minutes of heating was 87 ± 1 ºC, which was then maintained for the duration of the experiment. A water bath at ambient temperature was used to cool the gels to room temperature and the gels were incubated at ambient temperature for 1.5 hours. The gels were then de-moulded and soaked for 48 hours at room temperature respectively in 0.2 M β-mercaptoethanol (β-ME) to disrupt any disulfide bonds, 2 M urea to disrupt hydrogen bonds or 1 % (w/v) SDS to disrupt any ionic and hydrophobic interactions. Gels soaked in water were also used as controls.

The resulting gels were imaged using a camera with a resolution of 4032 x 3024 pixels. A black background was used for the ease of observation of transparency of the samples. The extent of contribution of different types of bond to the gel structure was analysed by conducting rheological frequency sweeps on soaked almond protein gels using a cone and plate geometry. The soaking process made the gels soft and highly deformable and also reduced their thickness. They were therefore loaded onto the rheometer, without any further manipulation. An optimized gap of 500 µm, based on preliminary experiments, was used to effectively fill the

geometry volume, as assessed visually. The G' value was observed as a function of frequency from 0.1 to 100 rad s^{-1} at a constant shear strain of 0.1 % (in the linear viscoelastic region) using a Discovery HR-2 Hybrid rheometer (TA Instruments). Three sets of gels were prepared on three independent days (n=3) and the results averaged.

2.6 Statistical analyses

Means were compared by one-way analysis of variance (ANOVA) using Minitab 18 software (Minitab LLC, Pennsylvania, USA) with a significance of 95 %, where applicable.

3. Results:

3.1 Protein yield and recovery

The almond protein isolate (API) obtained in this study had a high protein content (Table 1), with 94 ± 1 % protein and a protein yield of 23 ± 3 %, calculated on a dry basis for defatted almond flour. This is similar to the API obtained previously using saline borate buffer, where the protein content was 93 ± 2 % and the protein yield 27 ± 6 % (Sharma, et al., 2010).

3.2 Fundamental properties

3.2.1 Solubility and Z-potential

Protein solubility in aqueous solutions is a key functional property that influences other functional properties. In the present case, a typical U shaped solubility curve was observed with a solubility minimum of ~10 % of extracted almond protein occurring around pH 5.5 (Figure 1A), close to pH 5 reported in prior studies of API (Wolf, et al., 1998).

The solubility of the API in neutral to alkaline solutions (pH range 7-9) was high, ranging from 70-80 %. This solubility is similar to or slightly lower than other nut proteins, such as cashew and walnut proteins (~ 80 -90 %) (Hu, et al., 2017; Ogunwolu, Henshaw, Mock, Santros, & Awonorin, 2009), as well as popular legume proteins such as soy, pea and chickpea (70-90 %) (Ladjal-Ettoumi, Boudries, Chibane, & Romero, 2016; Nishinari, Fang, Guo, & Phillips, 2014).

In the acidic range (pH 3-4), almond protein solubility was also high ranging between 80-90 %. This contrasts with most plant protein isolates, including those from cashew, walnut, soy, pea and chickpea, which have minimal or low solubility (~ 10-50 %) in this pH range. The ability of the API extracted here to remain soluble across a broad range of pH makes the preparation a potentially versatile ingredient for use in acidic fruit or yoghurt-based drinks and/or in near neutral plant-based milk-like beverages.

The change in zeta-potential as a function of pH (Figure 1B) correlates with the solubility curve, with the iso-electric point of ~pH 5.5 consistent with the pH of minimal solubility. This is close to the reported broad iso-electric range of almond proteins (pH 3-5), with the values being a function of the extraction method employed to isolate almond proteins (de Souza, et al., 2020; Wolf, et al., 1998). Decreasing the pH from 9 to 3 changed the net surface charge from a negative maximum to a positive maximum, consistent with the gradual de-protonation of amino and carboxyl groups. Interestingly, it was observed that the net negative charge on the proteins at pH 7 was similar in magnitude (~24 mV) to the net positive charge at pH 4 (~ 22 mV), leading to similar solubilities.

3.2.2 Secondary structure

The shape of the CD spectrum obtained at pH 7 (Figure 1C) resembles amandin, the major almond storage protein, containing a strong positive peak at 192 nm and negative peak signals at 208 nm, 216 nm and 222 nm. The spectrum is also similar to that observed previously for the skim almond milk (Devnani, et al., 2020), indicating that the secondary structure of the almond proteins was maintained during the production of the API here.

On lowering the pH from 7 to 4, a shift occurred in the position of the maximum negative peak from 208 nm to 206 nm, along with a significant reduction in peak intensity at 193 nm (Figure 1C), both of which signify a decrease in α-helical content. A decrease in the α-helical content was also observed in the data deconvoluted with Dichroweb (16 ± 2 % at pH 4 c.f. 21 ± 2 % at pH 7), together with an increase in unordered structure (44 ± 4 % at pH 4 c.f. 34 ± 3 % at pH 7) ($p<0.05$). The β-sheet structure, however, remained near constant (44 ± 4 % at pH 7 c.f. 40 ± 5 % at pH 4).

3.2.3 SDS-PAGE

Electrophoresis, both under non-reducing and reducing conditions, indicated a change in the protein molecular weight distribution with pH (Figure 1D).

Under non-reducing conditions, a major band with a MW of ~60-63 kDa constituting ~65 % of the total protein was observed at pH 7 (Figure 1D, Lane 4). This has been previously identified as amandin (Sathe, 1992), which is a hexameric protein composed of 6 prunin subunits (Albillos, et al., 2008). The presence of SDS disrupts the non-covalent interactions (Schmid et al., 2017), dissociating the hexameric protein into prunin subunits ranging in MW of 60-66 kDa, which are then observed on the gel. A few other bands at 47 kDa, 44 kDa, 35

kDa, 32 kDa, 26 kDa and 24 kDa were also present, concordant with prior studies (Sathe, 1992).

Reducing the pH to 4 resulted in a degree of acid hydrolysis of the almond proteins, leading to the appearance of several smaller molecular weight protein subunits (Figure 1D, Lane 2). The proteins with a MW of ~ 43 kDa and ≤ 10 kDa constituted ~ 50% of the total proteins, with other lower intensity bands also occurring at 58 kDa, 56 kDa, 49 kDa, 34-39 kDa, 26-29 kDa and 18 kDa. Similar dissociation behaviour under acidic conditions has been noted previously for both plant-based proteins, such as soy (Thanh & Shibasaki, 1979; Zhao, Yuan, Luo, & Zhao, 2011) and animal-based proteins like β-lactoglobulin (Townend, Weinberger, & Timasheff, 1960). This dissociation was further found to be time-dependent, with a higher extent of smaller molecular weight subunits (12-14 kDa and 24 kDa) observed after 24 hours, (Figure S1, Lane 2, Supplementary Information), compared to 2 hours (Figure 1D, Lane 2). Proteinase inhibitors were not used in these preparations and endogenous proteinases could contribute to the observed hydrolysis but these proteinases were not detected by mass spectrometry as the most probable proteins in the preparation after 24 hours (Table S1, Supplementary Information).

Prunin fragments or amandin subunits were found in all major SDS-PAGE bands below 43 kDa at pH 4 by mass spectrometry after 24 hours (Figure S1, Lane 2 and Table S1, Supplementary Information). These fragments indicate that amandin dissociates and is cleaved by hydrolysis into several smaller proteins with a broad molecular weight distribution. This observation confirms prior findings that acid dissociation of amandin occurs at pH equal to or lower than pH 4 (Wolf, et al., 1998).

In the presence of a reducing agent, at neutral pH, amandin is known to dissociate into its acidic (37-40 kDa) and basic polypeptides (20-22 kDa) (Sathe, 1992), as occurred here (Figure 1D, Lane 5). This molecular weight distribution is different to that observed at pH 4 under reducing conditions, where the major bands appear to shift down to 31 kDa and 14 kDa (Figure 1D, Lane 3). Additional bands of significant intensity under these conditions include proteins at 26.5 kDa, 21 kDa and ≤ 10 kDa.

Overall, it can be concluded that although the solubility and magnitude of net charge for API are similar at both pH values (Figure 1A and B), the structure (Figure 1C) and molecular weight distribution clearly differ (Figure 1D). Lowering the pH to 4 induces a time-dependent structural rearrangement through protein unfolding and acid induced or proteolytic cleavage to

form smaller molecular weight subunits. This rearrangement in protein structure is expected to influence the functional properties of API.

3.3 Functional properties

3.3.1 Heat denaturation

At neutral pH the denaturation temperature of API was high, with a clear endothermic peak occurring at 81 ± 1 ºC (Figure 2A). This temperature is higher than the denaturation temperatures reported for albumin (~63 ºC) and globulin (~73 ºC) fractions of almond proteins (Zhang, et al., 2017). Denaturation temperatures are known to vary, due to differences in raw materials and the conditions used to extract proteins, with lower denaturation temperatures of 54-62 ºC observed for some fractions (Li, et al., 2018) and higher denaturation temperatures of 87-92 ºC for different extraction processes (Amirshaghaghi, et al., 2017) or systems containing native almond proteins, such as those occurring in almond milk (T_m~ 98 ºC) (Bernat, Chafer, Rodriguez-Garcia, Chiralt, & Gonzalez-Martinez, 2015). These variations in extraction methods are expected to alter the composition and concentration of proteins present in the API (Figure 1D), altering almond protein heat stability.

No endothermic peak was detected at pH 4 indicating that the proteins present were completely denatured. In general, it has been seen that highly acidic conditions (pH < 4) partially denature globulins, lowering the protein stability and hence their denaturation temperatures and heat capacities (Il'in, Semenova, Belyakova, Antipova, & Polikarpov, 2004; Renkema, Lakemond, de Jongh, Gruppen, & van Vliet, 2000). For instance, two endothermic transitions having reduced heat capacities were obtained at lower temperatures of 68 ºC and 82 ºC at pH 3.8 for soy glycinin, in contrast to one endothermic peak at 88 ºC at pH 7.6 (Renkema, et al., 2000).

3.3.2 Foaming capacity and stability

In general, both foaming capacity (FC) and foam stability (FS) were much higher at pH 4 than at pH 7 (Figure 2B). There was a 54 ± 5% increase in volume after mixing at pH 4, which was 1.7 times the increase in volume observed at pH 7 (32 ± 3%). Further, no significant reduction in foam volume was noticed at pH 4 within 1.5 hrs ($p > 0.05$) in contrast to the drop in foam volume of 80 % of the initial value observed at pH 7. This difference was potentially due to the presence of smaller molecular weight proteins present at pH 4 (Figure 1D) that offer greater flexibility and ease of re-arrangement on the air-water interface, as compared to the more compact higher molecular weight proteins (particularly amandin) present at pH 7.

The foaming capacity and stability at pH 7 observed here were 1.7 times higher and 2.6 times lower than previously observed at pH 6.46 (Sze-Tao, et al., 2000). Foam stability and capacity were also found to be ~3 times higher here than that at pH 5, as previously measured by Sze-Tao, et al. (2000), this is likely due to the higher solubility of almond proteins observed at pH 4 compared to pH 5 (Figure 1A) These differences though, could also be attributed to different methodologies used for protein extraction, which is expected to influence the protein composition (Figure 1D), as well as the conditions applied to induce foaming.

3.3.3 Viscosity

All API solutions behaved as non-Newtonian shear thinning fluids (Figure S2, Supplementary Information), regardless of their concentration or pH, probably due to the disruption of weak-interparticle linkages through forces generated during shear, as well as the ability of protein molecules to orient themselves in the direction of flow (Damodaran, 2008).

In general, at any given point of time, the apparent viscosity of almond protein solutions at pH 4 was greater than that at pH 7 (Figure 3). This was potentially due to acid induced denaturation at pH 4 (Figure 1C and D) that led to more open structures, with a higher hydrodynamic volume and exposed hydrophobic sites that could increase molecular interaction and entanglement. In short, protein swelling and association was much greater at pH 4 than at pH 7. This hypothesis is supported by dynamic light scattering data, as larger particles were observed at pH 4, in a broad, dynamic and polydisperse particle size distribution (Supplementary Information, Figure S3). Higher viscosities have also been observed under acidic (pH 3- 4) conditions, as compared to near neutral (pH 6-7) conditions, for other commonly used plant and dairy based protein isolates, such as soy and whey, although the magnitude greatly varies with protein type and concentration (Dissanayake, Ramchandran, & Vasiljevic, 2013; Kinsella & Kinsella, 1979; Rattray & Jelen, 1995).

At pH 7, no significant differences were detected in the apparent viscosity (0.030 ± 0.01 Pa.s) obtained at a shear rate of 1 s^{-1} with incubation time, at any concentration. The low apparent viscosity of almond proteins even at higher concentrations, is consistent with prior observations (Sharma, et al., 2010; Sze-Tao, et al., 2000), and is close to that of whey proteins (0.027 Pa.s) at similar concentration (10 %) (Dissanayake, et al., 2013), highlighting the potential for the possible utilisation of API as a protein supplement.

At pH 4, the apparent viscosity was found to depend on the age of the solution. A maximum in viscosity was observed at time t=0, i.e. immediately after pH adjustment, after which viscosity

declined (Figure 3). This could be attributed to proteins undergoing structural reorganization to regain their thermodynamic equilibrium, which was initially disturbed upon changing the initial pH of the colloidal solution from pH 7.2 to 4.

This change in apparent viscosity with time, was also found to be a function of protein concentration. The apparent viscosity at the lowest protein concentration of 3 % (0.08 ± 0.02 Pa.s), stabilised within 24 hours and remained steady without any further increase over the course of incubation ($p>0.05$) (Figure 3A). Conversely, the higher protein concentrations of 6 % and 9 % began to thicken after a certain time, with the time and extent of thickening being affected by concentration (Figures 3B and C). The solution containing 6 % protein had its lowest viscosity of 0.11 ± 0.01 Pa.s after 24 hours, which increased to 2.0 ± 0.6 Pa.s after 72 hours. The fastest and most extensive thickening was observed, however, in the 9 % protein solution, where viscosity increased from its lowest value of 0.2 Pa.s after four hours to 20 ± 7 Pa.s after 24 hours, resulting in a sticky, semi-solid gel.. Similar concentration and age dependency on apparent viscosity has been reported previously for whey proteins at acidic pH values <4, where increasing the protein concentration resulted in reduced thickening time and increased apparent viscosities (Rattray, et al., 1995).

Age thickening, is a commonly observed phenomenon in dairy systems such as whey protein powder (Rattray, et al., 1995), reconstituted skim/whole milk powders (Trinh, 2006) and UHT milk (Datta & Deeth, 2001). Different mechanisms have been proposed to explain this effect, which, depending on the treatment, may be a product of heat and/or acid induced denaturation and proteolysis. In this study, at pH 4, hydrolysis could have contributed to the gradual increase in viscosity during storage.

The thickening observed here can be advantageous, for production of high viscosity/ semi-solid acidic gel-like vegan food alternatives.

3.3.4 Gel formation and microstructure

Temperature sweeps were performed with solutions containing 9 % protein after 24 hours of incubation time at room temperature to further understand gel formation. This protein concentration is higher than the observed minimum concentration of 8 % required for thickening and gelling at pH 4, as determined in preliminary experiments. It is also greater than the lowest concentration required for heat induced gelation at neutral pH (4 %) reported previously for almond protein preparations under similar conditions (Albillos, et al., 2009; Sathe, et al., 1997).

The development of a gel structure occurred mainly during the cooling process of the temperature sweep, as shown in Figure 4. The final gel strengths after cooling were 12-15 times higher than the gel strength measured during the initial heating stage of the temperature sweep. No significant differences were noted in the final strengths of the gels obtained at either pH.

Subtle differences were observed in the heating profiles as a function of pH (Figure 4A). At pH 7, the storage modulus G' became greater than the loss modulus G" at a temperature of ~50 ^{o}C, marking the onset of gelation. A rapid increase in storage modulus G' was though, seen only at temperatures > 80 ^{o}C. This was consistent with the denaturation temperature of 81 ± 1 ^{o}C observed through differential scanning calorimetry (Figure 2A). In contrast, as the sample at pH 4 was a viscous semi-solid gel before heating (Section 3.3.3), the heating profile of this gel suggested structural rearrangement where existing bonds were broken and new molecular interactions established, resulting in a gel with reduced strength post the completion of heating.

Either heating or the combination of heating and lowering the pH altered the appearance and microstructure of the protein solution or gel (Figure 5). Prior to heating, the pH 7 sample was liquid at room temperature, containing protein and fat particles suspended in a water phase (Figure 5A &B, pH 7 unheated). Upon heating, this solution formed an opaque, white gel, having a highly porous gel structure, with little fat present within the interconnected protein network; as evident by CLSM (Figure 5A &B, pH 7 heated) and cryo-SEM (Figure S4, Supplementary Information). These characteristics represent a typical particulate type structure resulting from the random association of protein aggregates, obtained following heat induced denaturation. Similar structural features were evident in gels formed from skim almond milk in our previous study (Devnani, et al., 2020).

The microstructure of the pale-yellow, sticky, opaque gel obtained at pH 4 before heating, consisted of a dense continuous matrix observed by CLSM (Figure 5A &B, pH 4 unheated), perhaps formed by the association or aggregation of swollen proteins at this pH. This sample remained opaque when heated but the colour and microstructure was subtly altered, with smaller fat droplets present in a more continuous protein phase (Figure 5A &B, pH 4 heated). A honeycomb-like structure was obtained using cryo-SEM at this pH (Figure S4, Supplementary Information), likely due to development of an eutectic artefact during the sample etching step (Macdougall, Ong, Palmer, & Gras, 2019; Ong, et al., 2011).

3.3.5 Molecular interactions in gel formation

The unheated gel formed at pH 4 due to protein denaturation and proteolytic activity appeared to be partially reversible and stabilized by both covalent and non-covalent interactions. These gels visibly disintegrated in water, β-ME and urea, with partial dissolution in SDS (Figure 6, pH 4 unheated). Aggregated proteins were evident in the microstructural images of the gel that disintegrated in water (Figure S5), providing further evidence that disintegration was incomplete. The solution containing β-ME was the most transparent, followed by urea, indicating increased dissolution of the small molecular weight proteins after breakage of disulphide and hydrogen bonds, respectively. The undissociated gel fragments observed in the SDS solution, could also indicate disulphide or hydrogen bonds. The low viscosity of these solutions prevented a frequency sweep analysis to assess gel properties (Figure 7).

Heating affected the morphology (Figure 6) and the dissociation of gels in different reagents (Figure 7). The gels responded differently depending on pH, potentially due to the different protein structure and molecular associations formed on heating. At pH 4, the colour of the sample changed from pale yellow to light reddish-brown (Figure 6, pH 4 unheated and heated), while at pH 7, the gel had a cream colour (Figure 6, pH 7 heated). Though the storage moduli of gels formed at pH 4 and 7 following temperature sweeps were comparable (Figure 4), the strength of the gels immersed in water, measured after 48 hours of incubation at room temperature post batch heating (87 ^{o}C for 30 minutes) were significantly different; with the pH 7 gels appearing much stronger (~35X) as compared to the pH 4 gels (Figure 7).

There was no visible loss of structure in any of the reagent solutions following heating, unlike in unheated solutions (Figure 6). In presence of denaturation reagents, the lowest G' for the pH 4 gels was obtained in the presence of urea (Figure 7), indicating hydrogen bonds may stabilise the gel structure. In contrast, the gel strength increased after soaking in SDS compared to water (Figure 7), perhaps due to reduced overall electrostatic charge causing partial dewatering of the gel and a stronger association of the proteins under these conditions. Additionally, the released Na^{+} ions from SDS could further influence the ionic strength (Otzen, 2002), which is known to impact gel properties (Totosaus, Montejano, Salazar, & Guerrero, 2002). At pH 7, the gel strength was similar for heated gels placed in urea and β- ME solutions, implying that the hydrogen and disulphide bonds contributed equally to gel network formation and stabilisation at this pH. The lowest G' was obtained in the presence of SDS (Figure 7), suggesting that ionic and hydrophobic interactions also play a major role supporting the protein structure of these gels.

In conclusion, gels similar in strength, but different in structure and molecular interactions were obtained at both pH values. Future studies focusing on the viscoelastic properties of these gels and the comparison of their gel deformation behaviour to other plant protein gels formed under similar conditions, could provide interesting insights that may help to broaden the applicability of such gels into a variety of food applications.

Almond protein behaviour is expected to change as a function of extraction conditions (de Souza, et al., 2020; 2020; Sathe, et al., 2009; Sharma, et al., 2010), including extraction buffer (sodium borate was used here but alkaline extraction is a commercially relevant method). A future study may seek to compare the properties of gels formed from proteins extracted by different methods. The potential to control protein hydrolysis, either through the addition of proteinase inhibitors (Ayensa, Montero, Borderías, & Hurtado, 2002) or through the use of additional proteinases to hydrolyse proteins (Tavano, 2013) could also potentially be used to further examine the effect of protein structure and association on gel properties.

4. Conclusion

This study provides a better understanding of the impact of solution pH on the structure and behaviour of almond proteins, which have a relatively compact secondary structure and a higher molecular weight distribution at pH 7 than at pH 4. At these pH, almond proteins have a similar solubility owing to opposite but similar net charge. Structural differences, due to acid and potentially proteolytic hydrolysis at pH 4, resulted in enhanced foaming properties, greater viscosity and age dependant thickening. These preparations also respond differently to heat. While at pH 7, thermal denaturation was necessary to initiate protein aggregation and gelation; at pH 4, acid induced denaturation was sufficient to form a weak gel network. Stronger, thermo-irreversible gels with a higher gel strength were obtained at both pH values following heating. The microstructure and molecular interactions within these gels also appear to differ. These findings will assist the utilisation of almond proteins in food products of differing pH, where variation in protein size, extent of structural unfolding and denaturation lead to different molecular interactions and gel properties. These proteins also have potential utility in foaming, thickening and gel formation and this study illustrates the potential to tune almond preparations by varying pH and temperature to obtain a range of tailored products with desired properties.

Declaration of Competing Interest

The authors declare that they have no known competing financial interests or personal relationships that could have appeared to influence the work reported in this paper.

Acknowledgement

Ms Bhanu Devnani thanks The University of Melbourne for a Melbourne Research Scholarship. This research did not receive any specific grants from funding agencies in the public, commercial or not-for-profit sectors. Bhanu Devnani, Lydia Ong and Sally Gras were supported by The ARC Dairy Innovation Hub, a collaboration between The University of Melbourne, The University of Queensland and Dairy Innovation Australia Ltd. The authors thank The Advanced Microscopy Facility (AMF), The Biological Optical Microscopy Platform (BOMP), The Melbourne Protein Characterisation Facility and The Mass Spectrometry and Proteomics Facility at The Bio21 Molecular Science and Biotechnology Institute, and The Particulate Fluids Processing Centre at The University of Melbourne for access to equipment.

References:

Albillos, S. M., Jin, T., Howard, A., Zhang, Y., Kothary, M. H., & Fu, T. J. (2008). Purification, crystallization and preliminary X-ray characterization of prunin-1, a major component of the almond (*Prunus dulcis*) allergen amandin. *Journal of Agricultural and Food Chemistry*, 56(13), 5352-5358. http://doi.org/10.1021/jf800529k

Albillos, S. M., Menhart, N., & Fu, T. J. (2009). Structural stability of Amandin, a major allergen from almond (*Prunus dulcis*), and its acidic and basic polypeptides. *Journal of Agricultural and Food Chemistry*, 57(11), 4698-4705. http://doi.org/10.1021/jf803977z

Almond Board of California (2020). Almond Varieties and Selections: Evaluation of National and International Varieties or Selections Under Development

Aluko, R. E., Mofolasayo, O. A., & Watts, B. M. (2009). Emulsifying and foaming properties of commercial yellow pea (*Pisum sativum L.*) seed flours. *Journal of Agricultural and Food Chemistry*, 57(20), 9793-9800. http://doi: 10.1021/jf902199x

Amirshaghaghi, Z., Rezaei, K., & Rezaei, M. H. (2017). Characterization and functional properties of protein isolates from wild almond. *Journal of Food Measurement and Characterization*, 11(4), 1725-1733. https://doi.org/10.1007/s11694-017-9553-y

AOAC (2016). Official methods of analysis of AOAC International. Rockville, MD: AOAC International, ISBN: 978-0-935584-87-5.

Ayensa, M., Montero, M., Borderías, A. J., & Hurtado, J. L. (2002). Influence of some protease inhibitors on gelation of squid muscle. *Journal of Food Science*, 67(5), 1636-1641. https://doi.org/10.1111/j.1365-2621.2002.tb08697.x

Bernat, N., Chafer, M., Rodriguez-Garcia, J., Chiralt, A., & Gonzalez-Martinez, C. (2015). Effect of high pressure homogenisation and heat treatment on physical properties and stability of almond and hazelnut milks. *LWT-Food Science and Technology*, 62(1), 488-496. https://doi.org/10.1016/j.lwt.2014.10.045

Boye, J., Wijesinha-Bettoni, R., & Burlingame, B. (2012). Protein quality evaluation twenty years after the introduction of the protein digestibility corrected amino acid score method. *British Journal of Nutrition*, 108 Suppl 2(S2), S183-211. http://doi.org/10.1017/S0007114512002309

627 Calixto, F. S., Canellas, J., & de Toda, F. M. (1982). A chemical study of the protein fraction
628 of Mediterranean sweet almond varieties (*Prunus amygdalus*). *Zeitschrift für*
629 *Lebensmittel-Untersuchung und -Forschung A*, 175(1), 34-37.
630 https://doi.org/10.1007/BF01267829
631 Costa, J., Mafra, I., Carrapatoso, I., & Oliveira, M. B. (2012). Almond allergens: molecular
632 characterization, detection, and clinical relevance. *Journal of Agricultural and Food*
633 *Chemistry*, 60(6), 1337-1349. http://doi.org/10.1021/jf2044923
634 Damodaran, S., Parkin, K. L., & Fennema, O. R. (2008). Fennema's food chemistry. (4th ed.).
635 CRC press, (Chapter 5).
636 Datta, N., & Deeth, H. (2001). Age gelation of UHT milk—a review. *Food and Bioproducts*
637 *Processing*, 79(4), 197-210. https://doi.org/10.1205/096030801753252261
638 De Angelis, E., Bavaro, S. L., Forte, G., Pilolli, R., & Monaci, L. (2018). Heat and Pressure
639 Treatments on Almond Protein Stability and Change in Immunoreactivity after
640 Simulated Human Digestion. *Nutrients*, 10(11), 1679.
641 http://doi.org/10.3390/nu10111679
642 de Souza, T. S., Dias, F. F., Koblitz, M. G. B., & de Moura Bell, J. M. (2020). Effects of
643 enzymatic extraction of oil and protein from almond cake on the physicochemical and
644 functional properties of protein extracts. *Food and Bioproducts Processing*, 122, 280-
645 290. https://doi.org/10.1016/j.fbp.2020.06.002
646 Devnani, B., Ong, L., Kentish, S., & Gras, S. (2020). Heat induced denaturation, aggregation
647 and gelation of almond proteins in skim and full fat almond milk. *Food Chemistry*,
648 325, 126901. http://doi.org/10.1016/j.foodchem.2020.126901
649 Dissanayake, M., Ramchandran, L., & Vasiljevic, T. (2013). Influence of pH and protein
650 concentration on rheological properties of whey protein dispersions. *International*
651 *Food Research Journal*, 20(5), 2167-2171. Retrieved from
652 https://www.proquest.com/scholarly-journals/influence-ph-protein-concentration-on-
653 rheological/docview/1491101354/se-2?accountid=12372
654 Fulton, J., Norton, M., & Shilling, F. (2019). Water-indexed benefits and impacts of
655 California almonds. *Ecological Indicators*, 96, 711-717.
656 https://doi.org/10.1016/j.ecolind.2017.12.063
657 Gill, P., Moghadam, T. T., & Ranjbar, B. (2010). Differential scanning calorimetry
658 techniques: applications in biology and nanoscience. *Journal of Biomolecular*
659 *Techniques*, 21(4), 167. Retrieved from
660 https://www.ncbi.nlm.nih.gov/pmc/articles/PMC2977967/

House, J. D., Hill, K., Neufeld, J., Franczyk, A., & Nosworthy, M. G. (2019). Determination of the protein quality of almonds (*Prunus dulcis L.*) as assessed by in vitro and in vivo methodologies. *Food Science & Nutrition*, 7(9), 2932-2938. https://doi.org/10.1002/fsn3.1146

Hu, H., Fan, T., Zhao, X., Zhang, X., Sun, Y., & Liu, H. (2017). Influence of pH and salt concentration on functional properties of walnut protein from different extraction methods. *Journal of Food Science and Technology*, 54(9), 2833-2841. https://doi.org/10.1007/s13197-017-2721-6

Il'in, M. M., Semenova, M. G., Belyakova, L. E., Antipova, A. S., & Polikarpov, Y. N. (2004). Thermodynamic and functional properties of legumin (11S globulin from *Vicia faba*) in the presence of small-molecule surfactants: effect of temperature and pH. *Journal of Colloid and Interface Science*, 278(1), 71-80. http://doi.org/10.1016/j.jcis.2004.05.039

Joshi, A. U., Liu, C., & Sathe, S. K. (2015). Functional properties of select seed flours. *LWT-Food Science and Technology*, 60(1), 325-331. https://doi.org/10.1016/j.lwt.2014.08.038

Kendall, A., Marvinney, E., Brodt, S., & Zhu, W. (2015). Life cycle–based assessment of energy use and greenhouse gas emissions in almond production, part I: Analytical framework and baseline results. *Journal of Industrial Ecology*, 19(6), 1008-1018. https://doi.org/10.1111/jiec.12332

Kinsella, J. E. (1979). Functional properties of soy proteins. *Journal of the American Oil Chemists' Society*, 56(3 Part1), 242-258. https://doi.org/10.1007/BF02671468

Ladjal-Ettoumi, Y., Boudries, H., Chibane, M., & Romero, A. (2016). Pea, chickpea and lentil protein isolates: physicochemical characterization and emulsifying properties. *Food Biophysics*, 11(1), 43-51. https://doi.org/10.1007/s11483-015-9411-6

Laemmli, U. K. (1970). Cleavage of structural proteins during the assembly of the head of bacteriophage T4. *Nature*, 227(5259), 680-685. http://doi.org/10.1038/227680a0

Li, S., Chu, S., Lu, J., Wang, P., & Ma, M. (2018). Molecular and structural properties of three major protein components from almond kernel. *Journal of Food Processing and Preservation*, 42(3), e13536. https://doi.org/10.1111/jfpp.13536

Macdougall, P. E., Ong, L., Palmer, M. V., & Gras, S. L. (2019). The microstructure and textural properties of Australian cream cheese with differing composition. *International Dairy Journal*, 99, 104548. https://doi.org/10.1016/j.idairyj.2019.104548

695 Nishinari, K., Fang, Y., Guo, S., & Phillips, G. (2014). Soy proteins: A review on
696 composition, aggregation and emulsification. *Food Hydrocolloids*, 39, 301-318.
697 https://doi.org/10.1016/j.foodhyd.2014.01.013
698 Ogunwolu, S. O., Henshaw, F. O., Mock, H.-P., Santros, A., & Awonorin, S. O. (2009).
699 Functional properties of protein concentrates and isolates produced from cashew
700 (*Anacardium occidentale L.*) nut. *Food Chemistry*, 115(3), 852-858.
701 https://doi.org/10.1016/j.foodchem.2009.01.011
702 Ong, L., Dagastine, R. R., Kentish, S. E., & Gras, S. L. (2011). Microstructure of milk gel
703 and cheese curd observed using cryo scanning electron microscopy and confocal
704 microscopy. *LWT-Food Science and Technology*, 44(5), 1291-1302.
705 https://doi.org/10.1016/j.lwt.2010.12.026
706 Otzen, D. E. (2002). Protein unfolding in detergents: effect of micelle structure, ionic
707 strength, pH, and temperature. *Biophysical Journal*, 83(4), 2219-2230.
708 https://doi.org/10.1016/S0006-3495(02)73982-9
709 Rattray, W., & Jelen, P. (1995). Viscous behaviour of whey protein concentrate dispersions.
710 *International Dairy Journal*, 5(7), 673-684.
711 https://doi.org/10.1016/0958-6946(95)00018-X
712 Renkema, J. M., Lakemond, C. M., de Jongh, H. H., Gruppen, H., & van Vliet, T. (2000).
713 The effect of pH on heat denaturation and gel forming properties of soy proteins.
714 *Journal of Biotechnology*, 79(3), 223-230.
715 http://doi.org/10.1016/s0168-1656(00)00239-x
716 Sathe, S. K. (1992). Solubilization, electrophoretic characterization and in vitro digestibility
717 of almond (*Prunus amygdalus*) proteins *Journal of Food Biochemistry*, 16(4), 249-
718 264. https://doi.org/10.1111/j.1745-4514.1992.tb00450.x
719 Sathe, S. K., & Sze, K. (1997). Thermal aggregation of almond protein isolate. *Food*
720 *Chemistry*, 59(1), 95-99. https://doi.org/10.1016/S0308-8146(96)00180-X
721 Sathe, S. K., Venkatachalam, M., Sharma, G. M., Kshirsagar, H. H., Teuber, S. S., & Roux,
722 K. H. (2009). Solubilization and electrophoretic characterization of select edible nut
723 seed proteins. *Journal of Agricultural and Food Chemistry*, 57(17), 7846-7856.
724 http://doi.org/10.1021/jf9016338
725 Schmid, M., Prinz, T. K., Stäbler, A., & Sängerlaub, S. (2017). Effect of sodium sulfite,
726 sodium dodecyl sulfate, and urea on the molecular interactions and properties of whey protein
727 isolate-based films. *Frontiers in Chemistry*, 4, 49. https://doi.org/10.3389/fchem.2016.00049

Sharma, G. M., Su, M., Joshi, A. U., Roux, K. H., & Sathe, S. K. (2010). Functional properties of select edible oilseed proteins. *Journal of Agricultural and Food Chemistry*, 58(9), 5457-5464. http://doi.org/10.1021/jf1002446

Sreerama, N., & Woody, R. W. (2000). Estimation of protein secondary structure from circular dichroism spectra: comparison of CONTIN, SELCON, and CDSSTR methods with an expanded reference set. *Analytical Biochemistry*, 287(2), 252-260. http://doi.org/10.1006/abio.2000.4880

Su, M., Liu, C., Roux, K. H., Gradziel, T. M., & Sathe, S. K. (2017). Effects of processing and storage on almond (*Prunus dulcis L.*) amandin immunoreactivity. *Food Research International*, 100 (Part 1), 87-95. http://doi.org/10.1016/j.foodres.2017.06.061

Summo, C., Palasciano, M., De Angelis, D., Paradiso, V. M., Caponio, F., & Pasqualone, A. (2018). Evaluation of the chemical and nutritional characteristics of almonds (*Prunus dulcis* (Mill). DA Webb) as influenced by harvest time and cultivar. *Journal of the Science of Food and Agriculture*, 98(15), 5647-5655. http://doi.org/10.1002/jsfa.9110

Sze-Tao, K., & Sathe, S. (2000). Functional properties and in vitro digestibility of almond (*Prunus dulcis L.*) protein isolate. *Food Chemistry*, 69(2), 153-160. https://doi.org/10.1016/S0308-8146(99)00244-7

Tavano, O. L. (2013). Protein hydrolysis using proteases: An important tool for food biotechnology. *Journal of Molecular Catalysis B: Enzymatic*, 90, 1-11, https://doi.org/10.1016/j.molcatb.2013.01.011

Thanh, V. H., & Shibasaki, K. (1979). Major proteins of soybean seeds. Reversible and irreversible dissociation of beta-conglycinin. *Journal of Agricultural and Food Chemistry*, 27(4), 805-809. https://doi.org/10.1021/jf60224a024

Totosaus, A., Montejano, J. G., Salazar, J. A., & Guerrero, I. (2002). A review of physical and chemical protein-gel induction. *International Journal of Food Science & Technology*, 37(6), 589-601. https://doi.org/10.1046/j.1365-2621.2002.00623.x

Townend, R., Weinberger, L., & Timasheff, S. N. (1960). Molecular interactions in β-lactoglobulin. IV. The dissociation of β-lactoglobulin below pH 3.52. *Journal of the American Chemical Society*, 82(12), 3175-3179. https://doi.org/10.1021/ja01497a047

Trinh, B. (2006). Rheological characterisation of age thickening in milk concentrates (Doctoral dissertation, Massey University).

760 Whitmore, L., & Wallace, B. A. (2004). DICHROWEB, an online server for protein
761 secondary structure analyses from circular dichroism spectroscopic data. *Nucleic*
762 *Acids Research*, 32(suppl_2), W668-673. http://doi.org/10.1093/nar/gkh371
763 Wolf, W. J., & Sathe, S. K. (1998). Ultracentrifugal and polyacrylamide gel electrophoretic
764 studies of extractability and stability of almond meal proteins. *Journal of the Science*
765 *of Food and Agriculture*, 78(4), 511-521.https://doi.org/10.1002/(SICI)1097-
766 0010(199812)78:4<511::AID-JSFA148>3.0.CO;2-X
767 Yada, S., Lapsley, K., & Huang, G. (2011). A review of composition studies of cultivated
768 almonds: Macronutrients and micronutrients. *Journal of Food Composition and*
769 *Analysis*, 24(4-5), 469-480. https://doi.org/10.1016/j.jfca.2011.01.007
770 Yang, C., Wang, Y., Vasanthan, T., & Chen, L. (2014). Impacts of pH and heating
771 temperature on formation mechanisms and properties of thermally induced canola
772 protein gels. *Food Hydrocolloids*, 40, 225-236.
773 https://doi.org/10.1016/j.foodhyd.2014.03.011
774 Zhang, Q., Zhang, X., Feng, Y., & Shi, F. (2017). Compositions and Physicochemical
775 Properties of Sweet Almond Isolate Proteins. *Scientia Agricultura Sinica*, 50(13),
776 2564–2575. http://doi.org/10.3864/j.issn.0578-1752.2017.13.015
777 Zhao, M.-M., Yuan, B.-E., Luo, D.-H., & Zhao, Q.-Z. (2011). Subunit dissociation of
778 soybean protein isolates in acid conditions. *Journal of South China University of*
779 *Technology*, 39(9). http://doi.org/10.3969/j.issn.1000-565X.2011.09.005

780

FIGURE CAPTIONS

Figure 1: The fundamental properties of almond protein isolate (API) as a function of pH. (A) Solubility and (B) Zeta potential of API solutions at pH ranging from pH 3 to pH 9. (C) Circular dichroism spectra of API solutions at pH 4 (- -) and pH 7 (—). (D) Electrophoresis of API solutions, run after approximately 2 hours following solution preparation, where lane 1 contains a molecular weight ladder; lane 2 and 3 contain API solution at pH 4; and lane 4 and 5 contain API solution at pH 7, under non-reducing and reducing conditions respectively. The error bars in A and B represent the standard deviation (n=3) of the mean for three replicate experiments.

Figure 2: The functional properties of almond protein isolate (API) as a function of pH. (A) DSC thermograms and (B) foam stability of API solutions (1 % w/v) at pH 4 (grey) and pH 7 (black). The error bars in B represent the standard deviation (n=3) of the mean for three replicate experiments.

Figure 3: The time dependence of apparent viscosity (or consistency index at a shear rate of 1 s^{-1}) of almond protein isolate (API) as a function of pH. Apparent viscosity was measured at pH 4 (○) or pH 7 (●) at concentrations of 3 % (A), 6 % (B) or 9 % (C) respectively. The inset below (C) highlights the initial decrease in viscosity with time. The error bars represent the standard deviation (n=3) of the mean for two replicate experiments.

Figure 4: The temperature dependence of storage modulus G' (black symbols) and loss modulus G" (white symbols) during heating (A) and cooling (B) of almond protein isolate. Temperature sweeps of solutions of API were measured at pH 7 (▲, Δ) and pH 4 (●, ○) using a protein concentration of 9 %. The data is represented in arbitrary units (A.U.) as the cone and plate geometry applied used a non-standard gap of 1000 μm. The error bars represent the standard deviation (n=3) of the mean for three replicate experiments.

Figure 5: The appearance and microstructure of almond protein isolate (API) solutions and gels formed as a function of pH. Samples at pH 7 (left) and pH 4 (right) were examined before and after heating to 90 ºC followed by cooling to 25 ºC in a rheometer. (A) Digital camera images of API gels. (B) Two-dimensional confocal laser scanning microscopy images of API samples at each pH, where the fat is stained in red and the protein is stained in green. The scalebar in each of these confocal images is 25 μm in length.

Figure 6: The dissociation of almond protein isolate (API) gels in dissociation reagents, including water, β-Mercaptoethanol (β ME), sodium dodecyl sulfate (SDS) and urea (shown top). Images are shown for the gels formed from almond protein isolate (API) at a concentration of 9 % w/v, prepared at either pH 4 or pH 7 either without or with heating at 87 ± 1 ºC for 30 minutes (far left column). Images are also shown for gels that have been soaked in different dissociation reagents for 48 hours (four columns to right). Each glass dish is ~ 6 cm in diameter.

Figure 7: Storage modulus (G') of gels formed from almond protein isolate gels at a concentration of 9 % w/v, prepared at either pH 4 (▓) or pH 7 (▒), either with or without heating at 87 ± 1 ºC for 30 minutes. Select heated gels were also soaked in different solutions (indicated on the x axis) for 48 hours. Frequency sweeps were performed after 48 hours at a frequency of 1 Hz. The data is represented in arbitrary units (A.U.) as the cone and plate geometry applied used a non-standard gap of 500 μm. The error bars represent the standard deviation (n=3) of the mean for three replicate experiments.

Figure 1

A.

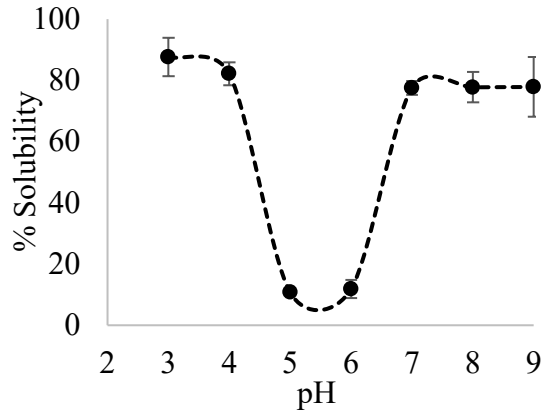

B.

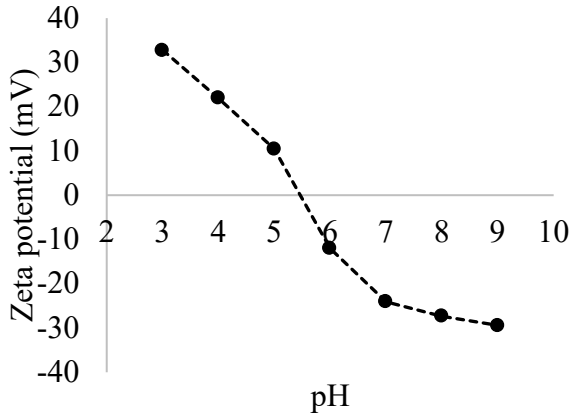

C.

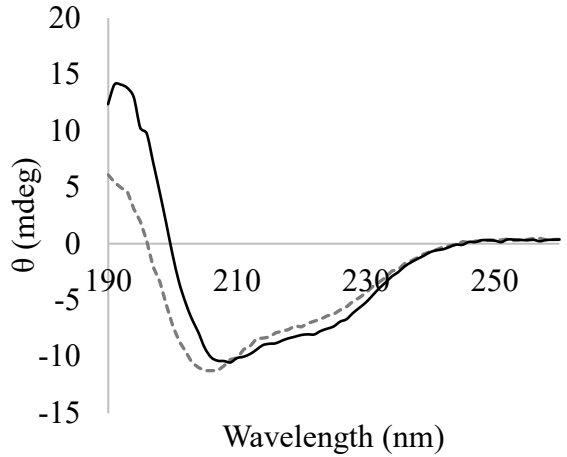

D.

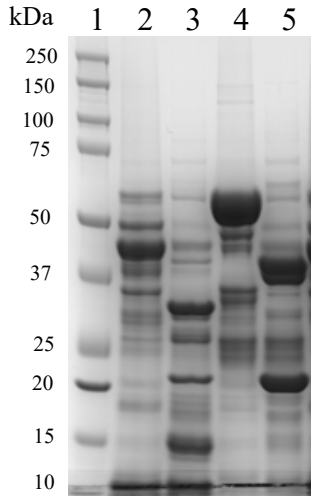

Figure 2

A.

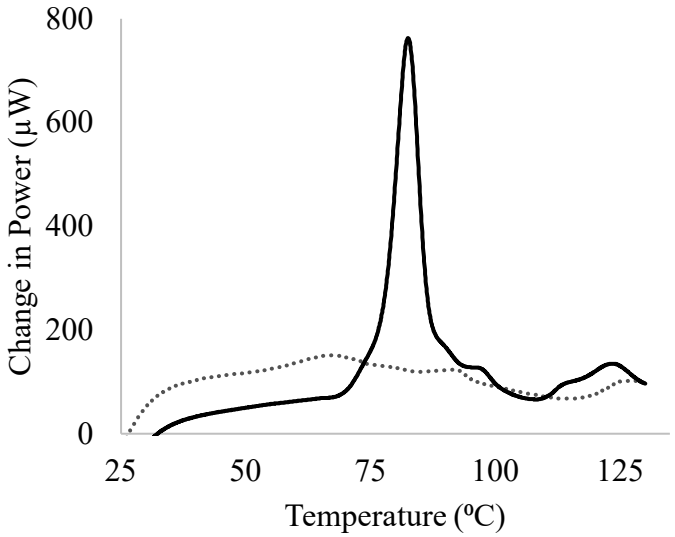
800
600
400
200
0
Change in Power (µW)
25
50
75
100
125
Temperature (ºC)

B.

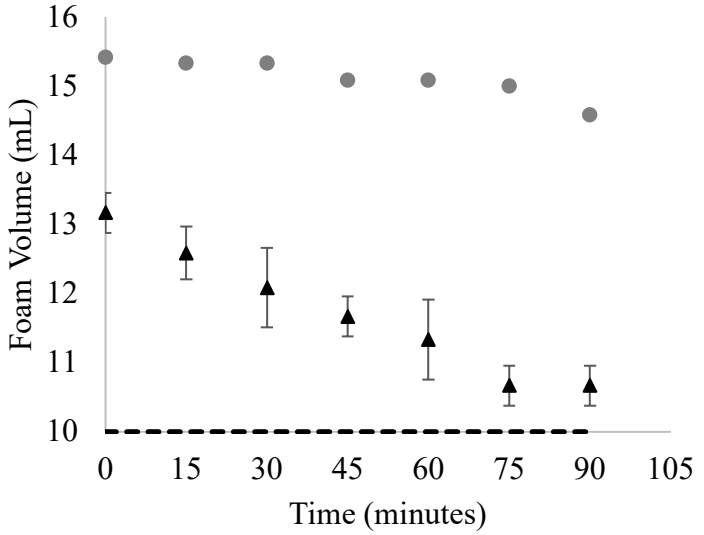
16
15
14
13
12
11
10
Foam Volume (mL)
0
15
30
45
60
75
90
105
Time (minutes)

Figure 3

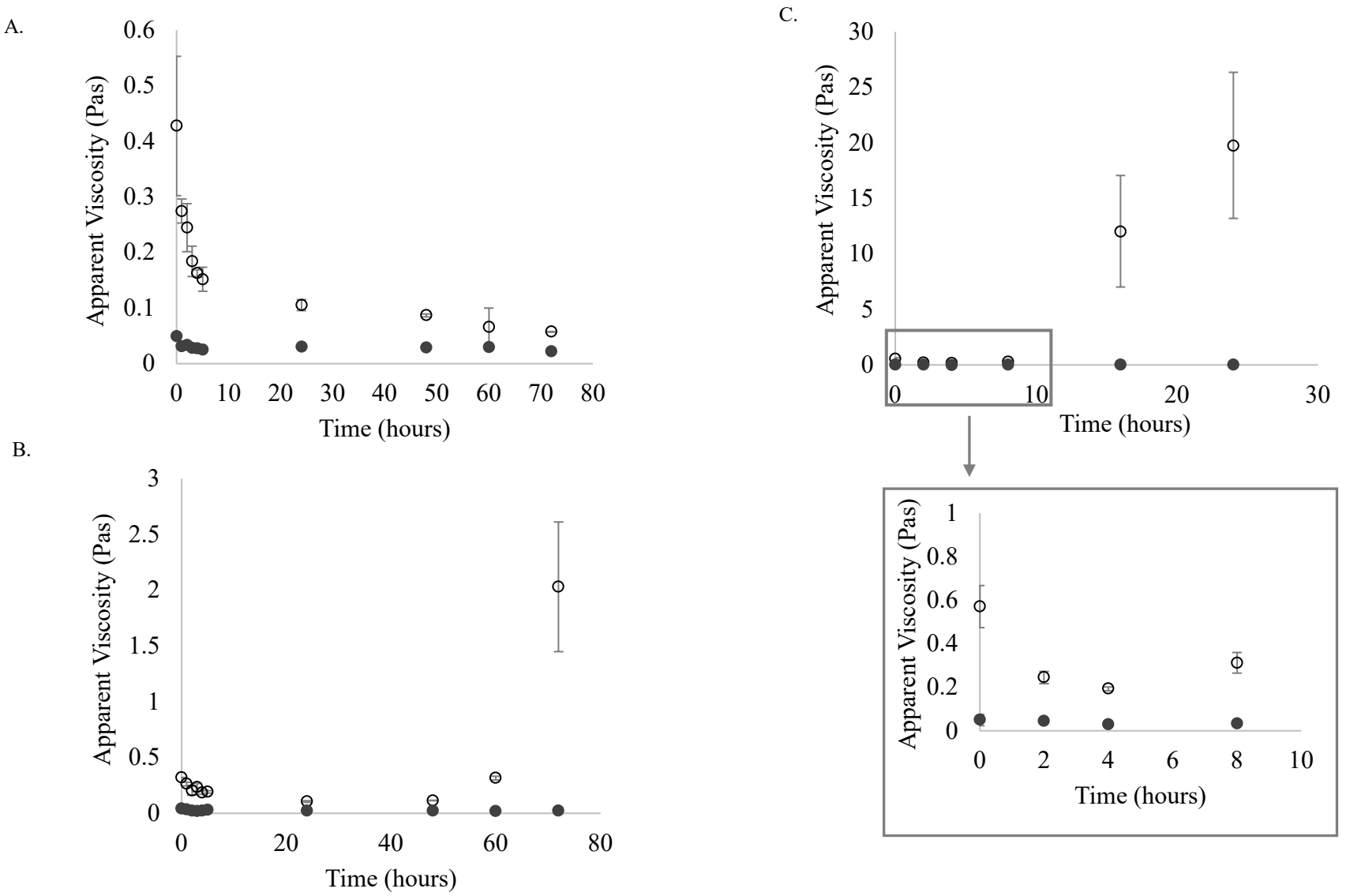
A.
Apparent Viscosity (Pas)
0.6
0.5
0.4
0.3
0.2
0.1
0
0 10 20 30 40 50 60 70 80
Time (hours)
B.
Apparent Viscosity (Pas)
3
2.5
2
1.5
1
0.5
0
0 20 40 60 80
Time (hours)
C.
Apparent Viscosity (Pas)
30
25
20
15
10
5
0
0 10 20 30
Time (hours)
Apparent Viscosity (Pas)
1
0.8
0.6
0.4
0.2
0
0 2 4 6 8 10
Time (hours)

Figure 4

A.

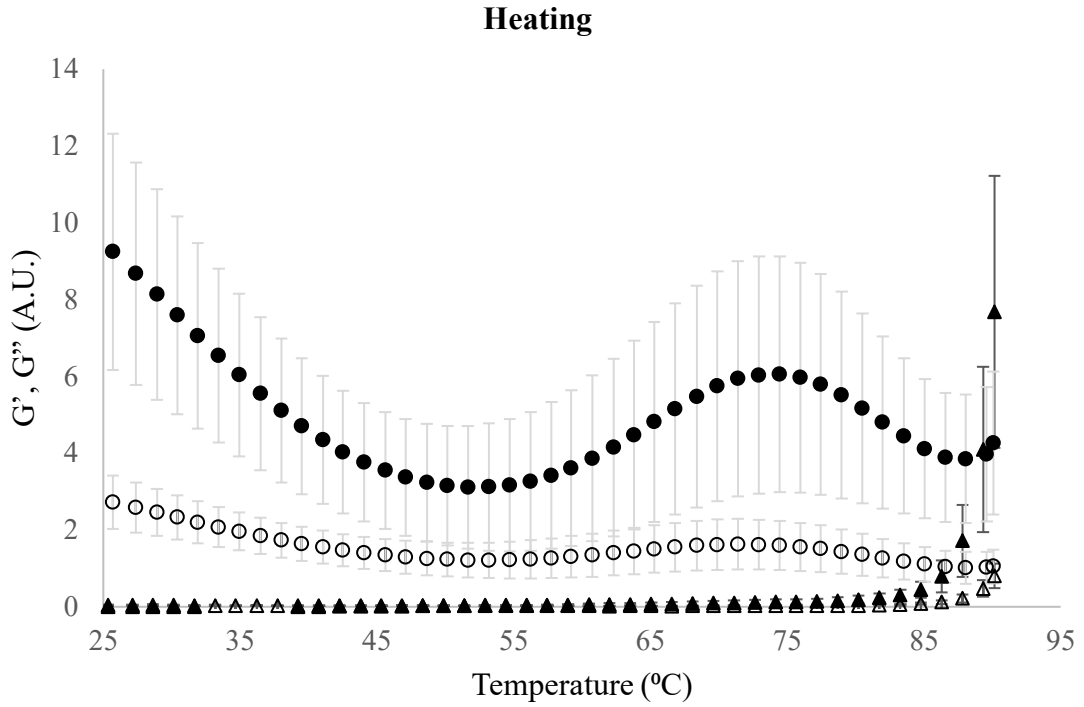
Heating
G', G" (A.U.)
14
12
10
8
6
4
2
0
25
35
45
55
65
75
85
95
Temperature (ºC)

B.

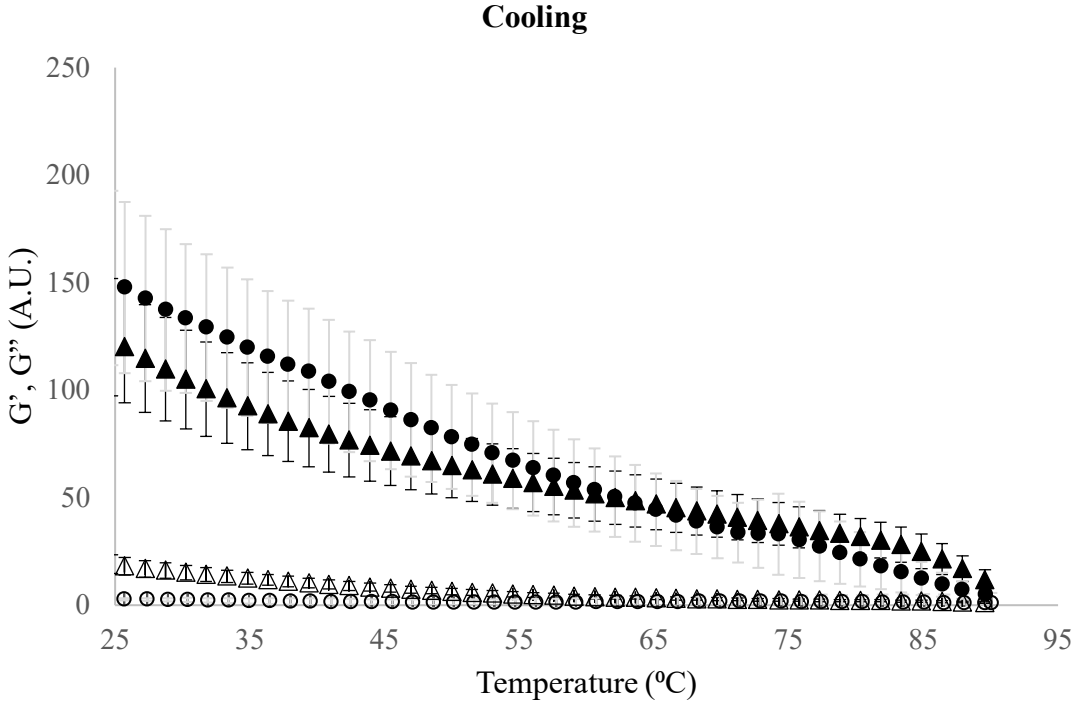
Cooling
G', G" (A.U.)
250
200
150
100
50
0
25
35
45
55
65
75
85
95
Temperature (ºC)

Figure 5

A.

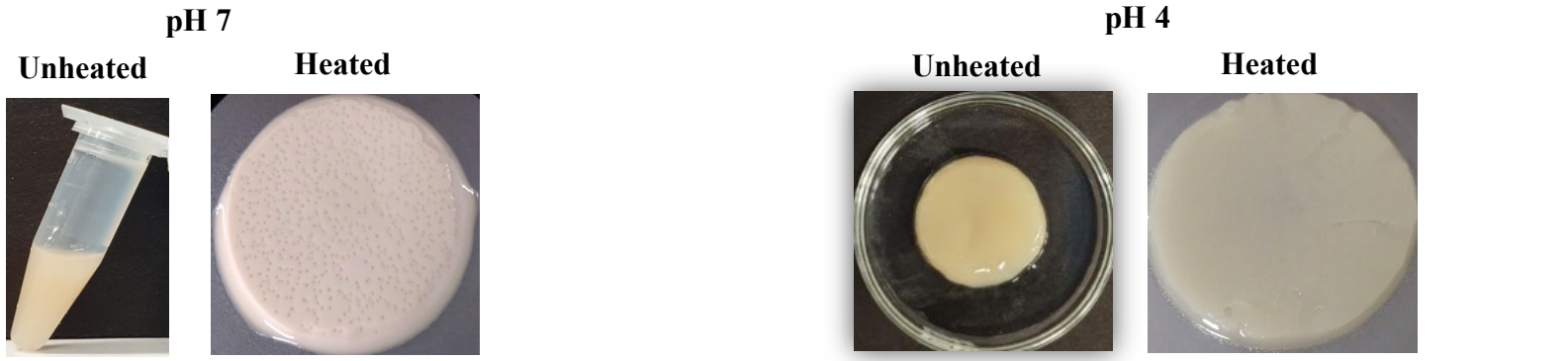

B.

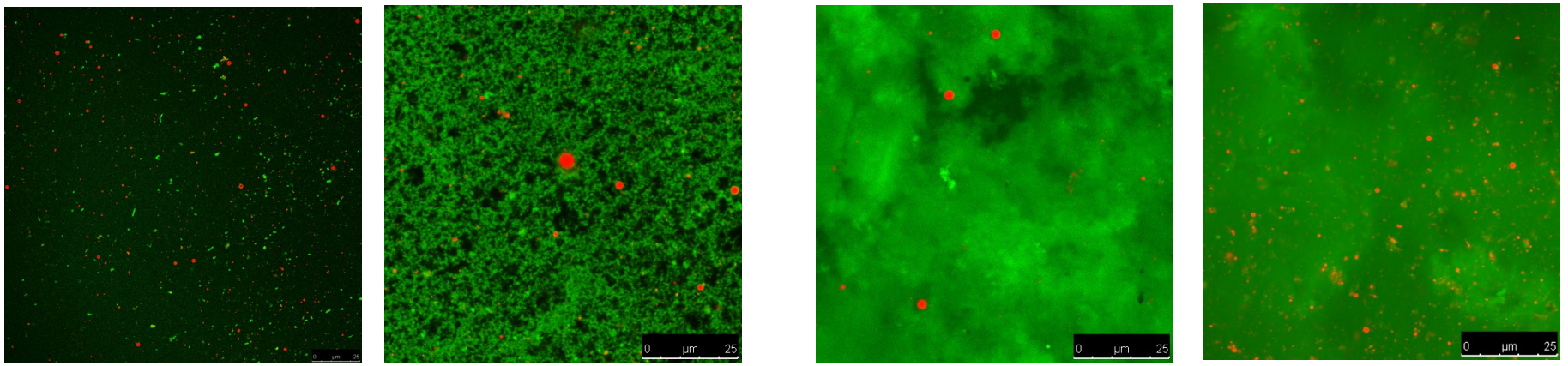

Figure 6

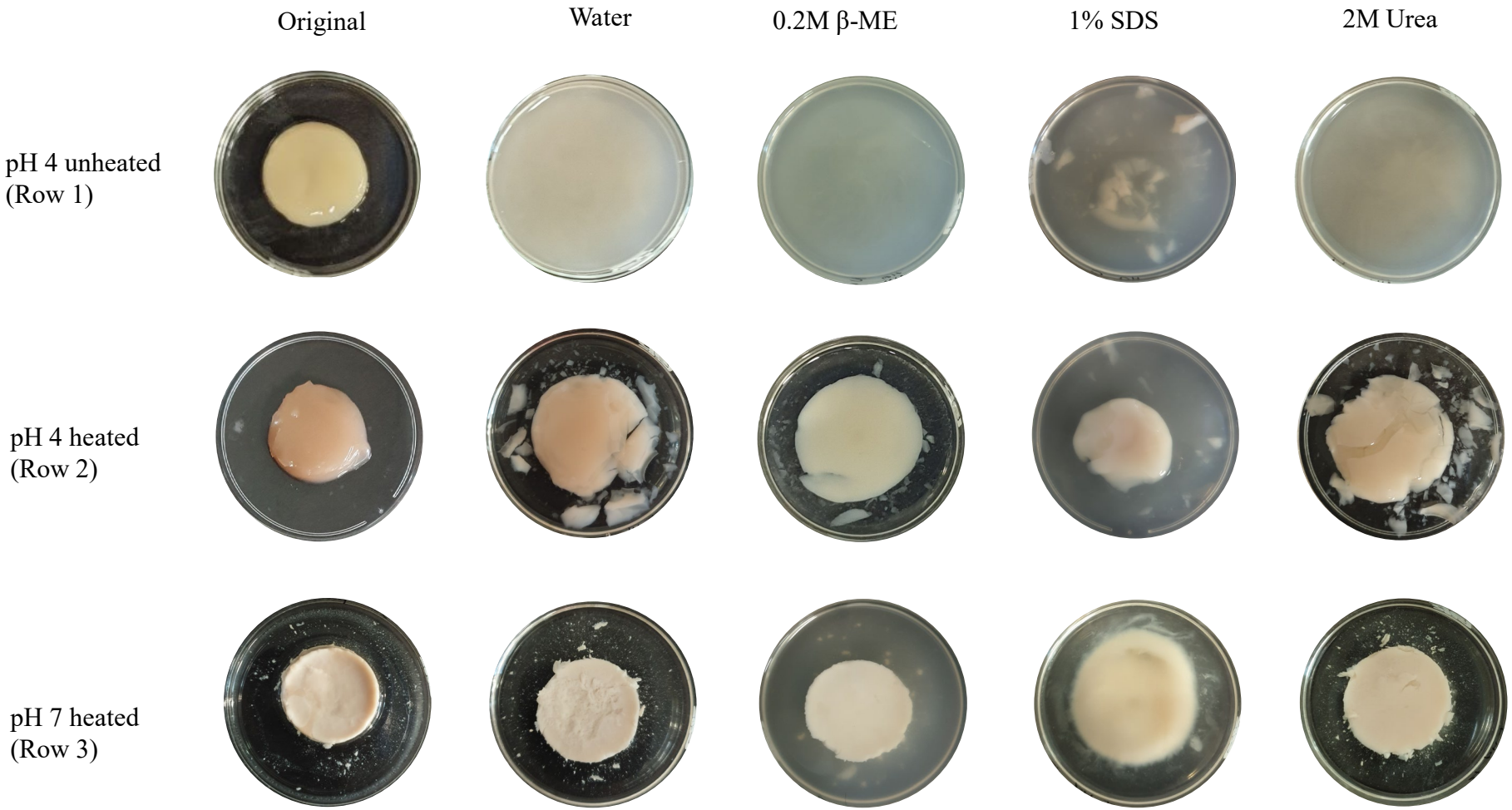
Original
Water
0.2M β-ME
1% SDS
2M Urea
pH 4 unheated (Row 1)
pH 4 heated (Row 2)
pH 7 heated (Row 3)

Figure 7

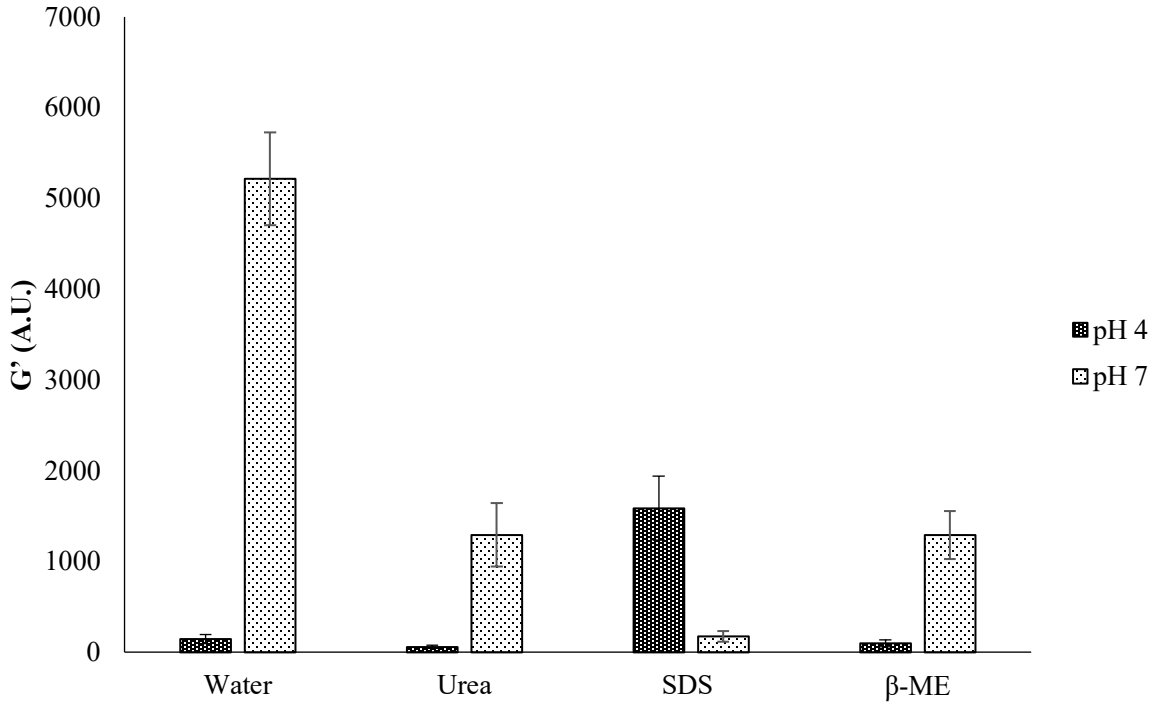
7000
6000
5000
4000
3000
2000
1000
0
G' (A.U.)
Water
Urea
SDS
β-ME
pH 4
pH 7